



**HAL**  
open science

## Irradiation effects on antibody performance in the frame of biochip-based instruments development for space exploration

M. Baqué, M. Dobrijevic, A. Le Postollec, Thibault Moreau, C. Faye, F. Vigier, S. Incerti, G. Coussot, J. Caron, O. Vandenabeele-Trambouze

### ► To cite this version:

M. Baqué, M. Dobrijevic, A. Le Postollec, Thibault Moreau, C. Faye, et al.. Irradiation effects on antibody performance in the frame of biochip-based instruments development for space exploration. *International Journal of Astrobiology*, 2017, 16 (1), pp.82-90. 10.1017/S1473550415000555 . hal-01285933

**HAL Id: hal-01285933**

**<https://hal.science/hal-01285933v1>**

Submitted on 18 Feb 2022

**HAL** is a multi-disciplinary open access archive for the deposit and dissemination of scientific research documents, whether they are published or not. The documents may come from teaching and research institutions in France or abroad, or from public or private research centers.

L'archive ouverte pluridisciplinaire **HAL**, est destinée au dépôt et à la diffusion de documents scientifiques de niveau recherche, publiés ou non, émanant des établissements d'enseignement et de recherche français ou étrangers, des laboratoires publics ou privés.

## Irradiation effects on antibody performance in the frame of biochip-based instruments development for space exploration

Baque M. <sup>1,\*</sup>, Dobrijevic M. <sup>2,3</sup>, Le Postollec A. <sup>2,3</sup>, Moreau T. <sup>4</sup>, Faye C. <sup>5</sup>, Vigier F., Incerti S. <sup>6,7</sup>, Coussot G. <sup>8</sup>, Caron J. <sup>9</sup>, Vandenabeele Trambouze Odile <sup>10,11,12</sup>

<sup>1</sup> Univ Roma Tor Vergata, Dept Biol, Rome, Italy.

<sup>2</sup> Univ Bordeaux, LAB, UMR 5804, F-33270 Florac, France.

<sup>3</sup> CNRS, LAB, UMR 5804, F-33270 Florac, France.

<sup>4</sup> Univ Clermont Ferrand, INSERM U1103, GReD, CNRS UMR6293, Aubiere, France.

<sup>5</sup> Cap Alpha, COLCOM, F-34830 Clapiers, France.

<sup>6</sup> Univ Bordeaux, CENBG, UMR 5797, F-33170 Gradignan, France.

<sup>7</sup> CNRS, IN2P3, CENBG, UMR 5797, F-33170 Gradignan, France.

<sup>8</sup> Univ Montpellier, Inst Biomol Max Mousseron, Fac Pharm, CNRS, Unite Mixte Rech 5247, F-34093 Montpellier 5, France.

<sup>9</sup> Inst Bergonie, Dept Radiotherapy, Ctr Comprehens Canc, F-33076 Bordeaux, France.

<sup>10</sup> Univ Bretagne Occidentale, LMEE, UEB, IUEM UMR 6197, Plouzane, France.

<sup>11</sup> CNRS, IUEM UMR 6197, LMEE, Plouzane, France.

<sup>12</sup> IFREMER, UMR6197, LMEE, Plouzane, France.

\* Corresponding author : M. Baqué, email address : [mickael.baque@gmail.com](mailto:mickael.baque@gmail.com)

### Abstract :

Several instruments based on immunoassay techniques have been proposed for life-detection experiments in the framework of planetary exploration but few experiments have been conducted so far to test the resistance of antibodies against cosmic ray particles. We present several irradiation experiments carried out on both grafted and free antibodies for different types of incident particles (protons, neutrons, electrons and C-12) at different energies (between 9 MeV and 50 MeV) and different fluences. No loss of antibodies activity was detected for the whole set of experiments except when considering protons with energy between 20 and 30 MeV (on free and grafted antibodies) and fluences much greater than expected for a typical planetary mission to Mars for instance. Our results on grafted antibodies suggest that biochip-based instruments must be carefully designed according to the expected radiation environment for a given mission. In particular, a surface density of antibodies much larger than the expected proton fluence would prevent significant loss of antibodies activity and thus assuring a successful detection.

**Keywords** : astrobiology, biochip, cosmic rays, search for extraterrestrial life

## 51 **1. Introduction**

52 Among the next tools to search for signs of past or present life in our Solar System,  
53 several instruments based on the biochip technology have been proposed in the  
54 framework of planetary exploration. A biochip is a miniaturized device composed of  
55 molecular recognition tools (or affinity receptors) like antibodies (Baqué *et al.* 2011b;  
56 de Diego-Castilla *et al.* 2011; Parro *et al.* 2005, 2011a; Sims *et al.* 2005, 2012) or  
57 aptamers (Baqué *et al.* 2011a), which allows the detection of hundreds of different  
58 compounds in a single assay. Widely developed for biotechnology use and medical or  
59 environmental diagnostics (see for example Wang 2006), miniaturized instruments  
60 based on biochips have been indeed proposed and studied for biosignature detection in  
61 an astrobiological context since more than 15 years (McKay *et al.* 2000; Parro *et al.*  
62 2005; Le Postollec *et al.* 2007; Sims *et al.* 2005).

63 Mars, one of the most probable planetary body where to find signs of extinct or extant  
64 life outside of Earth, is the target of many upcoming dedicated missions: ESA-  
65 Roscosmos' ExoMars rover in 2016-2018, NASA's Mars2020 rover (a follow-up of to  
66 the Curiosity rover) and the Icebreaker mission concept proposed for a 2021 launch to  
67 be part of NASA's Discovery program (McKay *et al.*, 2013). Different space  
68 instruments based on the biochip technology and using antibodies have been proposed  
69 for these future missions: the Life Marker Chip (LMC) (Martins 2011; Sephton *et al.*  
70 2013; Sims *et al.* 2012), and the Signs Of Life Detector (SOLID) (Parro *et al.* 2005,  
71 2008, 2011a, 2011b). Another project, the Biochip for Organic Matter Analysis in  
72 Space (BiOMAS), proposes to combine both antibodies and aptamers in a single  
73 instrument (Baqué *et al.* 2011b, 2011a; Le Postollec *et al.* 2007). Recently, first in the  
74 framework of Mars2020 announcement of opportunity, and then in the framework of  
75 NASA's Discovery 2014 announcement of opportunity, these different teams have

76 united to work on the SOLID instrument proposal for the Icebreaker mission and thus to  
77 contribute with their different expertise to improve the technological readiness level of a  
78 biochip-based instrument for space exploration (Manchado *et al.* 2015; McKay *et al.*  
79 2013; Smith & Parro 2014).

80 Indeed, although biochips are known to be very sensitive tools to detect specific target  
81 molecules, their sensitivity is related to the presence of functional affinity receptors. In  
82 order to develop a “space biochip”, it is thus necessary to ensure that these biological  
83 receptors will survive space hazards. In particular, due to the very sparse data on this  
84 topic, it is important to determine the behavior of these biological receptors under  
85 cosmic particles irradiation.

86 Le Postollec *et al.* (2009a) performed simulations with the Geant4 Monte Carlo toolkit  
87 in order to estimate the radiation environment that a biochip would face if it were placed  
88 into a rover dedicated to explore Mars’ surface. Ionizing doses accumulated and fluxes  
89 of particles entering the biochip have been established for both the Earth-Mars transit  
90 and the journey on Mars’ surface. Neutrons and gammas appear as dominant radiation  
91 species on Mars’ soil whereas protons dominate during the interplanetary travel. These  
92 results have been confirmed by other studies done by McKenna-Lawlor *et al.* (2012)  
93 and Derveni *et al.* (2012). Moreover, these simulations can today be confronted to the  
94 real radiation environment of an actual mission to Mars as it was monitored by the  
95 Radiation Assessment Detector (RAD) instrument on-board the Mars science laboratory  
96 spacecraft on cruise to Mars and continue to be recorded by the rover Curiosity directly  
97 on its surface (Hassler *et al.* 2013; Kim *et al.* 2014; Zeitlin *et al.* 2013). Indeed, the total  
98 cosmic radiation dose rate of  $210 \pm 40 \mu\text{Gy/day}$  (Hassler *et al.* 2013) recorded at Gale  
99 Crater by Curiosity and the one measured inside the Mars Science Laboratory  
100 spacecraft during its cruise to Mars ( $481 \pm 80 \mu\text{Gy/day}$ ) (Zeitlin *et al.* 2013) proved to

101 be in the same order of magnitude as model predictions with respectively  $\sim 840 \mu\text{Gy/day}$   
102 (without any shielding) for the Martian surface and  $\sim 240 \mu\text{Gy/day}$  for the Earth-Mars  
103 transit considering only GCR (galactic cosmic rays) contribution (Le Postollec *et al.*  
104 2009a).

105

106 Considering the lack of experimental data about cosmic rays effect on antibodies,  
107 particularly under lyophilized (freeze-dried) state, our team decided to investigate the  
108 effects of different types of particles at several energies. Our objective is first to study  
109 and measure cosmic rays effects on biological receptors and second to define well-  
110 adapted protections for a biochip-based instrument if we find evidences that cosmic rays  
111 might have deleterious effect on their performances. In a first study, Le Postollec *et al.*  
112 (2009b) performed neutrons irradiation on both antibodies and fluorescein dyes (used  
113 for detection of recognition events) at two energies (0.6 and 6 MeV) and with different  
114 fluences. Sample analyses demonstrated that, in tested conditions, neutrons do not affect  
115 antibody recognition capability and fluorescence dye intensity. More recently, the  
116 effects of 2 MeV protons on antibody performances (Baqué *et al.* 2011b) were  
117 investigated. These studies showed that this irradiation process did not affect the  
118 performances of antibodies as molecular recognition tools. In addition, printed antibody  
119 and Alexa-647 fluorescent dye were demonstrated to be stable between 1.18 and 1.33  
120 MeV gamma radiation (de Diego-Castilla *et al.* 2011). Finally, Derveni *et al.* (2012)  
121 tested five antibodies freeze-dried in a variety of protective molecular matrices and  
122 exposed to 50 MeV protons. They showed that at a representative Mars-mission-dose,  
123 none of the antibodies studied exhibited any evidence of activity loss due to the  
124 radiation.

125 In the present paper, we broaden these previous studies to test the effect of electrons,  
126 carbon ions, protons (at different energies) and neutrons (at higher energies) on the  
127 recognition capability of antibodies (summarized in Fig 1). As protons and neutrons  
128 dominate the radiation environment during the Earth-Mars transit and on the Martian  
129 surface, we tested different high-energy particles from 15 to 50 MeV at different  
130 fluences. Moreover, other damaging particles are significantly present in cosmic and  
131 solar radiations such as carbon ions and electrons.

132 Chemicals and biological materials used to perform the experiments are given in section  
133 2. Section 3 describes samples preparation, particles irradiation parameters and analysis  
134 protocols. Results are presented in section 4. The last section draws conclusions on this  
135 study.

136

## 137 **2. Material**

138 Monoclonal anti-Horseradish Peroxydase antibodies were obtained from Antibodies-  
139 online (Germany), Horseradish peroxydase (type II), O-Phenylenediamine  
140 dihydrochloride (OPD),  $\text{NaH}_2\text{PO}_4$ , Tween® 20, sodium acetate, sucrose, sodium azide,  
141  $\text{NaOH}$ ,  $\text{H}_2\text{O}_2$ , BSA, (L)-Histidine and (D)-Arginine L-tyrosinamide, fluorescein and  
142 Tris(hydroxymethyl) aminomethane were purchased from Sigma Aldrich (Saint-  
143 Quentin, France).  $\text{NaCl}$  and  $\text{MgCl}_2$  were obtained from Chimie-Plus laboratoires  
144 (Bruyères de Pouilly, France) and Panreac Quimica (Barcelona, Spain), respectively.

145 Chemicals were analytical grade and were used as received. DNA-Bind™ plates were  
146 obtained from Corning (Netherlands) and Maxisorp™ plates were obtained from VWR  
147 (France). Optical density of the reaction products was measured on a Tecan Infinite  
148 M200 microplate reader (Lyon, France) at 492 nm.

149

### 150 **3. Method**

#### 151 **3.1. Sample preparation**

152 Our Biochip models are small polymer containers, called micro-wells, where antibodies  
153 samples are placed for the experiments. DNA-Bind™ plates were used for covalent  
154 grafting (N-Oxysuccinimide functionalization allows random amine binding, Moreau *et*  
155 *al.* 2011) whereas Maxisorp™ ones were used as sample containers for free antibodies.  
156 The samples preparation was done following the same protocol as in Baqué *et al.*  
157 (2011a).

158 Briefly, antibodies were irradiated under two different states: grafted and free. All  
159 samples were freeze-dried using the freeze-drying buffer described in Baqué *et al.*  
160 (2011a,b) and then sealed in a FoodSaver™ bag in dry atmosphere (silica gel was added  
161 in the bag) and stored in the dark at 4°C before irradiation. All irradiation effects were  
162 estimated on freeze-dried samples.

163

#### 164 **3.2. Irradiation parameters**

##### 165 **3.2.1. Conditioning of samples during irradiation**

166 In order to prevent potential degradations due to environmental changes (contact with  
167 air, moisture, potential organic contaminants, etc.), all samples were irradiated under  
168 their protecting packaging.

169 Micro-wells were irradiated directly in their sealed bags. The effect of the sealed bag,  
170 considering its thickness and composition, was assessed using simulations performed  
171 with the Geant4 toolkit (Agostinelli *et al.* 2003; Allison *et al.* 2006). We determined  
172 that the influence of the bag during irradiations was negligible as very few particles  
173 were stopped by this additional plastic layer and very few secondary particles were  
174 created (data not shown).

175

176 **3.2.2. Methodology adopted to choose irradiation parameters**

177 Numerical simulations give a basis to select the types of particles, energies and fluences  
178 that we have to consider for irradiation experiments. However, this choice mainly  
179 depends on technical constraints and the availability of irradiation facilities. As an  
180 example, it is generally not possible to conduct ground-based experiments with the very  
181 low flux of particles and the long duration of irradiation (months or years) encountered  
182 in interplanetary space. In addition, due to analysis constraints (limit of detection,  
183 uncertainties), it is also necessary to choose adequate irradiation parameters to ensure  
184 that potential effects of particles on our targets will be measurable.

185 In the present study, when possible, we have chosen to use fluences in the same order of  
186 magnitude as the surface density of grafted antibodies. The objective of our experiments  
187 was to study the interaction between different types of particles and the antibody  
188 molecule. Indeed, we wanted to determine if some particles could have a “direct effect”  
189 on the recognition molecule: when a particle interacts with the molecule, is there  
190 degradation or is the molecule completely insensitive to particle interaction? This  
191 approach can allow the identification of particles and energies more deleterious to  
192 antibodies (if existing) and the results obtained could help for studying the  
193 implementation of biochips on further exploration missions whatever the target object in  
194 the Solar System. For instance, it could give precious data on the shielding design that  
195 must be developed considering the expected irradiation environment.

196

197 To determine the density of antibodies grafted into a well, we used an innovative  
198 quantification technique called ADECA (Coussot *et al.* 2011a; Coussot *et al.* 2011b;  
199 Moreau *et al.* 2011) that was well adapted to our purpose. The grafting density of



200 antibodies was defined around  $8.8 \times 10^{11}$  antibodies/cm<sup>2</sup> with roughly  $2.8 \times 10^{11}$   
201 antibodies on the bottom and  $5 \times 10^{11}$  antibodies on the sidewalls.

202

203 The fluence of particles reaching the antibodies was assessed using numerical  
204 simulations performed with the Geant4 toolkit. Indeed, considering the geometry of the  
205 well, it is obvious that antibodies grafted on the sides do not receive the same fluence of  
206 particles as antibodies located at the bottom of the well. With a fluence of  $3 \times 10^{12}$   
207 particles/cm<sup>2</sup>, the fluence of particles on the sidewalls was derived from the Geant4  
208 simulations to be  $2.4 \times 10^{-2}$  times the total fluence so  $7.2 \times 10^{10}$  particles/cm<sup>2</sup>.  
209 Therefore, we can assess that 41% of antibodies grafted in a well have a significant  
210 chance to interact with at least one particle. With this method, direct effects of particles  
211 on antibodies can be detected if existing.

212 Lower fluences and higher fluences were also tested in some cases, with for example a  
213 fluence of protons ten times lower ( $3 \times 10^{11}$  particles/cm<sup>2</sup>) or a fluence of neutrons ten  
214 times higher ( $3 \times 10^{13}$  particles/cm<sup>2</sup>). In these cases, we estimate that 13% and 74% of  
215 grafted antibodies interacted with a particle respectively.

216 Free antibody samples were prepared at a concentration of  $15 \times 10^{16}$  antibodies/well.  
217 The exact disposition of antibodies into the well is not defined but it is assumed that  
218 they form several layers at the bottom of the well during freeze-drying. Therefore it is  
219 not possible to determine the number of antibodies that could interact with incident  
220 particles since each particle can penetrate in a column of piled antibodies.

### 221 **3.2.3. Neutron irradiation**

222 Neutron irradiation was performed at the cyclotron of Louvain-la-Neuve, in Belgium.

223 The high flux neutron irradiation facility uses a primary 50 MeV deuteron beam on a

224 beryllium target. The energy spectrum of the outgoing neutron beam is dominated by  
225 a peak in the region of 23 MeV. The mean energy of neutrons is 16.56 MeV.

226 The current was set to 7  $\mu$ A. Samples were positioned at two different distances so that  
227 they received two different fluences. At a 12 cm distance, the fluence was  $F_H = 3 \times 10^{13}$   
228 neutrons/cm<sup>2</sup> and the diameter of the beam was about 4.2 cm for 80% of homogeneity.  
229 Whereas at a 40.5 cm distance, the fluence was  $F_L = 3 \times 10^{12}$  neutrons/cm<sup>2</sup> and the  
230 diameter of the beam was about 10.2 cm for 80% of homogeneity. Samples were  
231 irradiated during approximately 22 minutes.

### 232 **3.2.4. Proton irradiation**

233 Proton irradiation was also performed at the cyclotron of Louvain-La-Neuve, on the  
234 Light Ion Facility (LIF) (Fig. 2 Top). This mono-energetic proton beam line can  
235 produce up to  $10^9$  protons/cm<sup>2</sup>/s with energies from 10 to 75 MeV (Berger *et al.* 1997).

236 The beam diameter is set to 10 cm and a  $\pm 10\%$  of homogeneity is ensured.

237 Three irradiation campaigns took place between June 2010 and June 2012. Our samples  
238 were irradiated with five different energies: 14.4 MeV, 20.9 MeV, 25.9 MeV, 29.4 MeV  
239 and 50.5 MeV. The proton flux was set to  $5 \times 10^8$  protons/cm<sup>2</sup>/s so that the irradiations  
240 lasted 1h40min to reach the fluence of  $3 \times 10^{12}$  protons/cm<sup>2</sup> for all the tested energies  
241 and 10min to reach  $3 \times 10^{11}$  protons/cm<sup>2</sup> for 25.9 MeV and 50.5 MeV.

### 242 **3.2.5. Electron irradiation**

243 Electron irradiation was performed at the Institut Bergonié (Bordeaux, France) (Fig. 2  
244 Bottom Left). The beam was calibrated to deliver 9 MeV electrons and it was scanned  
245 through a square collimator of 6 cm side. Samples were positioned at 1 m from the  
246 source. The flux delivered by the facility was 200 MU (Monitor Unit) per minute with 1  
247 MU corresponding to  $5.38 \times 10^6$  electrons impacting the bottom of the well (Gobet *et al.*

248 Submitted; unpublished data). Therefore, to deal with reasonable irradiation durations,  
249 we decided to irradiate samples during 70 minutes corresponding to a fluence of  $2.35 \times$   
250  $10^{11}$  electrons/cm<sup>2</sup>.

251

### 252 **3.2.6. Carbon ions irradiation**

253 Carbon ions irradiation was performed at the LNS (Laboratori Nazionali del Sud)  
254 facility of the INFN (Istituto Nazionale di Fisica Nucleare) in Catania. Samples were  
255 presented vertically in front of the beam. A specific mask was designed to fix the ELISA  
256 plate containing samples on a mobile device (Fig. 2 Bottom right) so that the whole  
257 plate could be irradiated at once without any intervention in the irradiation room.

258 The beam was scanned through a square collimator of 17 mm side. Calibration for the  
259 delivered dose has been done by means of a parallel plate ionization chamber.

260 Radiochromic films have been also used for minimizing gaps and overlaps between  
261 irradiated areas in order to ensure a homogeneous irradiation of all samples.

262 The beam delivered <sup>12</sup>C ions with an energy of 62 MeV/nuc. For this experiment, the  
263 fluence applied was different from other experiments as it was not reasonable to reach  $3$   
264  $\times 10^{12}$  carbon ions per cm<sup>2</sup> in an adequate delay and safe conditions. Therefore, we  
265 decided to study if energetic carbon ions could have an indirect effect on antibodies, i.e.  
266 if those particles of such energy could interact with the sample environment so that it  
267 could destabilize the whole system and degrade antibodies recognition performances.

268 The fluence was set to  $2.16 \times 10^6$  particles/cm<sup>2</sup> and was determined using results  
269 obtained with CREME 96 by Le Postollec *et al.* (2009a): it corresponds to the flux of  
270 <sup>12</sup>C 62 MeV/nuc ions at 1 A.U. (Astronomical Unit) delivered during 18 months  
271 (representing an upper limit for a Mars mission). The irradiation of each square area

272 lasted less than 20 seconds to reach the requested fluence so that the whole plate was  
273 irradiated within about 15 minutes.

274

### 275 **3.3. Analysis protocol**

#### 276 **3.3.1. Antibodies**

277 After irradiation, analyses were performed in order to define the irradiation effects on  
278 the antibody performance. Protocols used here were detailed in previous studies (Baqué  
279 *et al.* 2011a) and are summarized below.

280

281 Grafted antibodies were analyzed with a direct ELISA test (Baqué *et al.* 2011a). This  
282 method, called A2HRP, focuses only on the recognition capability of the antibody's  
283 antigen binding site (epitope) and does not give an insight on the degradation of the  
284 entire antibody structure (Moreau *et al.* 2011). Briefly, the number of active antigen  
285 binding sites was measured by quantifying the amount of antigen (HRP) specifically  
286 retained by the antibodies. Indeed, the amount of HRP could be easily quantified using  
287 external standards of free HRP as we have demonstrated that the enzymatic reactivity of  
288 HRP was identical for free HRP, or HRP complexed to both free or grafted antibody  
289 (Moreau *et al.* 2011).

290

291 Free antibodies were analyzed with a competitive ELISA test (Baqué *et al.* 2011a).  
292 Briefly, in micro-well plates with freshly grafted anti-HRP antibodies, a defined amount  
293 of HRP is placed in competition with diluted amounts of irradiated samples or controls.  
294 After washing, the amount of HRP measured in the micro-well is inversely proportional  
295 to the amount of active antibody in the sample. Based on competitive curves, we  
296 calculated the half maximal inhibitory concentration (IC<sub>50</sub>). In our experiment, this

297 concentration represents the amount of competitive antibody that should be added to  
298 inhibit 50% of antigen binding to grafted antibodies. Between two competitive  
299 experiments, both HRP and grafted antibody concentrations are maintained identical.  
300 Thus IC50 values are influenced by the affinity of competitive antibodies for the HRP.  
301 If the apparent affinity of competitive antibodies is reduced, then the IC50 measured  
302 will increase.

### 303 **3.3.2. Reference samples**

304 To evaluate the possible irradiation effects on our samples, different references and  
305 controls were prepared. Irradiation effect on antibody was evaluated by comparing  
306 irradiated samples to non-irradiated controls (NIC). NIC were treated simultaneously  
307 and in the same manner as the irradiated samples, though they were not submitted to  
308 irradiation. In order to estimate the effects of transport, temperature cycles and light  
309 exposure on biochip performances, reference samples were used. These reference  
310 samples (R4°C) were prepared at the same time as irradiated samples and NIC and were  
311 stored in the laboratory at 4°C in the dark until analysis. As described by Baqué *et al.*  
312 (2011a), all of the antibodies were freeze-dried using a specific buffer, which maintains  
313 the anti-HRP antibody recognition capabilities after freeze-drying and during storage to  
314 liquid reference levels. Results for grafted antibodies are therefore presented as  
315 percentages of active antibodies for more clarity and in order to normalize all acquired  
316 data during the several irradiation campaigns. This percentage is calculated by taking  
317 the amount of HRP retained by NIC to 100%. NIC and R4°C were confronted for each  
318 campaign to reflect any damage caused by transport, handling etc.

### 319 **3.3.3. Statistical treatment**

320 Irradiation effects were evaluated by comparing the mean signal values obtained for  
321 non-irradiated controls (NIC) and for irradiated samples. Thus, Student's t-tests were  
322 used to compare irradiated samples distribution and references distribution, taking into  
323 account the number of repetitions (from 4 to 18) and the standard deviation (SD) of  
324 each distribution. The differences between these two distributions were considered  
325 statistically significant with a 95 % level of confidence when the calculated  $p$ -values  
326 were below the 0.05 threshold value.

327

## 328 **4. Results**

### 329 **4.1. Grafted antibodies**

330 All the experiments performed on grafted antibodies are summarized in Table 1. This  
331 table presents the type, energy and fluence of particles tested. It also specifies the  
332 antibody grafting surface density allowing an assessment of the percentage of antibodies  
333 receiving at least one particle for each tested fluence. The percentage of antibodies still  
334 active after irradiation, calculated against non-irradiated controls (NIC), reveals possible  
335 degradation induced only by radiation exposure. Indeed, the effects of transport  
336 conditions are evaluated by confronting NIC with reference samples stored in the  
337 laboratory (R4°C), as described in paragraph 3.2.2. However, as for all the tested  
338 conditions NIC proved to be significantly equal to R4°C (not shown), only irradiation  
339 effects are presented here.

340 Irradiation on the other hand had different effects on the tested antibodies. Indeed,  
341 although no effect was detected with neutrons, electrons and  $^{12}\text{C}$ , significant effects  
342 were observed with protons. Surprisingly, for high fluences, protons between 20 and 30  
343 MeV significantly altered the antibody recognition performances, with losses around  
344 30-35% and  $p$ -values between  $10^{-4}$  and  $10^{-8}$ , but not at lower and higher energies.  
345 Similarly, even at a lower fluence 25 MeV protons produced a significant recognition

346 loss, though limited to only 10-20%, whereas at 50 MeV no significant recognition loss  
347 was recorded. In our model the antibody surface density was maintained identical for  
348 the different exposure experiments therefore only 13% of antibodies should have  
349 received at least one particle at the lowest proton fluence against 42% at the highest.  
350 The protons' energy appears thus as a more damaging factor than the fluence, as only a  
351 certain energy range (20-30 MeV) produced significant damage to antibodies regardless  
352 of the fluence applied. However, by diminishing the ratio between the antibody surface  
353 density and the particles' fluence by a factor 3 (42% against 13% of antibodies  
354 receiving at least one particle between high and low fluences respectively) the effect of  
355 irradiation was greatly attenuated for 25 MeV protons (65% against 84% of active  
356 antibodies respectively).

357 The other tested particles did not induce significant changes in antibody recognition  
358 capabilities even at very high neutron fluence ( $3 \times 10^{13}$  particles/cm<sup>2</sup>) or with heavy  
359 carbon ions at high energy (62MeV/n).

360

#### 361 **4.2. Free antibodies**

362 Free antibodies were irradiated by 25 MeV and 50 MeV protons and 17 MeV neutrons  
363 at different fluences ( $3 \times 10^{11}$  and  $3 \times 10^{12}$  particles/cm<sup>2</sup> for protons and  $3 \times 10^{12}$  and  $3 \times$   
364  $10^{13}$  particles/cm<sup>2</sup> for neutrons). Results are summarized in Table 2. The irradiation  
365 effect was estimated following the methodology described in Baqué *et al.* (2011a).  
366 Briefly, when the half maximal inhibitory concentration (IC50) significantly increases,  
367 it indicates that in average, the antibodies have lost recognition capabilities since HRP  
368 has only one epitope to which the antibody binds (Moreau *et al.* 2011).

369

370 No modification of free antibody recognition capabilities under proton irradiations at 50  
371 MeV was observed. However, at 25 MeV, we highlight here a significant recognition  
372 capability loss for free antibodies, leading to a significant increase in IC50 compared to  
373 the NIC. The increase in IC50 value indicates that, in average, the antibody activity has  
374 been deteriorated by 25 MeV protons irradiation leading to partial or complete antigen  
375 recognition site degradation. Based on a simplistic model, which considers that IC50  
376 changes are only linked to a total loss of recognition capability, we can however  
377 estimate the percentage of active antibodies compared to non-irradiated controls as  
378 reported in Table 2. A maximum of 50% of antibodies appear to have lost their  
379 recognition capability when irradiated with a high fluence of 25 MeV protons. Although  
380 the other recorded changes in IC50 values after proton or neutron irradiation appear also  
381 quite high, with 20 to 30 % damaged antibodies (most notably after a high neutron  
382 flux), they were not significantly different from the controls. These results however  
383 point out a high variability in the samples, which can be problematic for repeatability  
384 measurements of future space instruments.

385

## 386 **5. Discussion/Conclusion**

387

388 Based on Monte Carlo simulations of the radiation environment faced by a biochip  
389 dedicated to explore Mars' surface (Le Postollec *et al.* 2009a), our team performed  
390 several ground-based irradiation experiments on biochip recognition molecules. Even  
391 though protons and neutrons clearly dominate the radiation spectrum during the Earth-  
392 Mars transit and on the Martian surface, other particles might be equally deleterious to  
393 biological molecules such as the antibodies used in biochips. Furthermore, a wide range  
394 of particle energy and fluence can be considered according to the envisaged mission to



395 Mars but also to other planetary bodies of interest in the Solar System. In the present  
396 study, the irradiation effects of protons, neutrons, electrons and carbon ions on the  
397 recognition capabilities of antibodies were therefore investigated at different energies  
398 and fluences. Two antibodies formulations were submitted to irradiation in order to  
399 broadly represent any future biochip-based space instruments as both grafted and free  
400 antibodies are considered. Our experimental approach consisted of using particle  
401 fluences in the same order of magnitude as grafted antibodies surface density in order to  
402 measure any damaging effect occurring when a particle interacts with an antibody.

403 Among the tested particles, only protons significantly altered the antibodies recognition  
404 capabilities. These damaging effects were however recorded only for a certain energy  
405 range between 20 and 30 MeV at both high and low fluences but confirmed for both  
406 formulations (free and grafted antibodies). Indeed, at higher and lower protons energies  
407 the antibodies recognition capabilities were not significantly altered. Irradiations of free  
408 antibodies lead moreover to a high variability in the estimated recognition capabilities  
409 of our antibodies samples.

410 Therefore, although the energy range of deleterious particles appears quite limited, a  
411 biochip instrument performance would not be affected for a typical mission to Mars, as  
412 the fluences of particles in this energy range will be significantly lower than the  
413 antibody surface density. However, this result underlines that attention must be paid to  
414 the ratio between antibody surface density and particles fluences expected for a given  
415 mission. The biochip instrument must be designed so that antibody surface density is  
416 much greater than incident protons fluence. Instrument shielding and/or antibodies  
417 grafting density should be consequently adapted.

418

419 In a similar ground-based study performed on five antibodies freeze-dried in different  
420 protective molecular matrices, Derveni *et al.* (2012) pointed out the more damaging role  
421 of processing and packaging than irradiation. Using doses of protons and neutrons at  
422 high energies (50 and 47 MeV respectively), comparable to the ones used in the present  
423 work, they did not detect any evidence of activity loss due to irradiation for a typical  
424 mission dose ( $10^{11}$  to  $10^{12}$  protons/cm<sup>2</sup> and  $10^7$  to  $10^8$  neutrons/cm<sup>2</sup>). However, using  
425  $10^{13}$  protons/cm<sup>2</sup>, most of the antibodies lost their activity. Thanks to these results they  
426 suggested that further shielding or alternative radiation protection approaches would  
427 need to be considered for long duration missions to other astrobiological targets. Our  
428 present work confirms this suggestion. We propose that the ratio between the fluence of  
429 protons and the surface density of antibodies has to be much lower than unity to prevent  
430 important loss of activity.

431

432 The main limitation of ground-based studies is that each constraint is generally studied  
433 individually and for a limited period of time that is not representative of a real space  
434 mission. In particular, the effect of cosmic rays is generally studied at a given energy (or  
435 a limited range of energies) and for one type of particle in a single experiment.

436 Moreover, additional constraints and hazards are expected for a space instrument. Long  
437 term storage, temperature variations, contamination risks, launch, landing and  
438 transportations vibrations and shocks should all be taken into account in the design and  
439 testing of a space dedicated instrument. For these reasons, a real space exposure of  
440 biochip prototypes has been attempted in the past by the LMC team for a short-term  
441 mission aboard the BIOPAN platform on a Russian Foton spacecraft (Derveni *et al.*  
442 2013) and ground-based and field studies have been performed for the SOLID prototype  
443 (Parro *et al.* 2008; Sobrado *et al.* 2014). Furthermore, in the frame of the BiOMAS

444 project, biochip samples are currently exposed to real space conditions inside the  
445 EXPOSE-R2 platform of ESA, part of the Photochemistry on the Space Station (PSS)  
446 project, which was installed on the outside of the Zvezda module of the International  
447 Space Station (ISS) in August 2014 (Vigier *et al.* 2013).

448 The long-duration exposure of the EXPOSE missions (Rabbow *et al.* 2009, 2012, 2015)  
449 range from 12 to 18 months in the LEO environment of the ISS. The radiation  
450 environment at this altitude, although not equivalent to interplanetary space or the  
451 Martian surface, will allow anyway for a much better estimate of the long-term  
452 resistance of immunoassays instruments for space applications.

453 Nevertheless, due to the high number of potentially hazardous factors encountered  
454 during a space mission, ground-based studies are essential to isolate the most damaging  
455 ones and thus propose adequate shielding or handling procedures.

456

457 Thus, our results from ground-based irradiation campaigns globally indicate that cosmic  
458 rays might not alter the final performance of a biochip-based instrument in a typical  
459 Martian mission, when antibodies are used as binders to detect the presence or the  
460 absence of a target compound. The damaging effects of 20-30 MeV protons recorded in  
461 the present study should not however be overlooked and further testing on-ground will  
462 be necessary to support and interpret data from real space exposure missions.

463

464

#### 465 ***Acknowledgments***

466 The research leading to these results has received funding from the European Union  
467 Seventh Framework Programme FP7/2007-2013 under Grant Agreement no 262010 –  
468 ENSAR.

469 We would like to thank the French National Space Agency (CNES) (Convention  
470 number DCT/SI/IM/2009-17733) and the Interdisciplinary CNRS program  
471 “Environnements Planétaires et Origines de la Vie” for financial support.

472 We also thank the Louvain-la-Neuve cyclotron facility staff, the Institut Bergonié staff  
473 and the staff from the Laboratori Nazionali del Sud of the Istituto Nazionale di Fisica  
474 Nucleare for their help during irradiation experiments.

475

Proof For Review

476 **References**

477

- 478 Agostinelli, S. *et al.* (2003) Geant4—a simulation toolkit. *Nucl. Instrum. Methods*  
479 *Phys. Res. Sect. Accel. Spectrometers Detect. Assoc. Equip.* **506**(3), 250–303.
- 480 Allison, J. *et al.* (2006) Geant4 developments and applications. *IEEE Trans. Nucl. Sci.*  
481 **53**(1), 270–278.
- 482 Baqué, M. *et al.* (2011a) Investigation of Low-Energy Proton Effects on Aptamer  
483 Performance for Astrobiological Applications. *Astrobiology*. **11**(3), 207–211.
- 484 Baqué, M., Le Postollec, A., Coussot, G., Moreau, T., Desvignes, I., Incerti, S.,  
485 Moretto, P., Dobrijevic, M., & Vandenabeele-Trambouze, O. (2011b) Biochip  
486 for astrobiological applications: Investigation of low energy protons effects on  
487 antibody performances. *Planet. Space Sci.* **59**(13), 1490 – 1497.
- 488 Berger, G., Ryckewaert, G., Harboe-Sorensen, R., & Adams, L. (1997) Cyclone—A  
489 multipurpose heavy ion, proton and neutron test site. In *1997 RADECS*  
490 *Conference Data Workshop*. p. 51.
- 491 Coussot, G., Faye, C., Ibrahim, A., Ramonda, M., Dobrijevic, M., Postollec, A.,  
492 Granier, F., & Vandenabeele-Trambouze, O. (2011) Aminated dendritic  
493 surfaces characterization: a rapid and versatile colorimetric assay for estimating  
494 the amine density and coating stability. *Anal. Bioanal. Chem.* **399**(6), 2295–  
495 2302.
- 496 Coussot, G., Perrin, C., Moreau, T., Dobrijevic, M., Postollec, A.L., & Vandenabeele-  
497 Trambouze, O. (2011) A rapid and reversible colorimetric assay for the  
498 characterization of aminated solid surfaces. *Anal. Bioanal. Chem.* **399**(3), 1061–  
499 1069.
- 500 Derveni, M., Allen, M., Sawakuchi, G.O., Yukihiro, E.G., Richter, L., Sims, M.R., &  
501 Cullen, D.C. (2013) Survivability of Immunoassay Reagents Exposed to the  
502 Space Radiation Environment on board the ESA BIOPAN-6 Platform as a  
503 Prelude to Performing Immunoassays on Mars. *Astrobiology*,  
504 130103060450009.
- 505 Derveni, M., Hands, A., Allen, M., Sims, M.R., & Cullen, D.C. (2012) Effects of  
506 Simulated Space Radiation on Immunoassay Components for Life-Detection  
507 Experiments in Planetary Exploration Missions. *Astrobiology*. **12**(8), 718–729.
- 508 de Diego-Castilla, G., Cruz-Gil, P., Mateo-Martí, E., Fernández-Calvo, P., Rivas, L.A.,  
509 & Parro, V. (2011) Assessing Antibody Microarrays for Space Missions: Effect  
510 of Long-Term Storage, Gamma Radiation, and Temperature Shifts on Printed  
511 and Fluorescently Labeled Antibodies. *Astrobiology*. **11**(8), 759–773.
- 512 Gobet, F. *et al.* (Submitted) Experimental and Monte Carlo absolute characterization of  
513 a medical electron beam. *Radiat. Meas.*

- 514 Hassler, D.M. *et al.* (2013) Mars' Surface Radiation Environment Measured with the  
515 Mars Science Laboratory's Curiosity Rover. *Science*, 1244797.
- 516 Kim, M.-H.Y. *et al.* (2014) Comparison of Martian Surface Radiation Predictions to  
517 the Measurements of Mars Science Laboratory Radiation Assessment Detector  
518 (MSL/RAD). In American Geophysical Union Fall 2014 Meeting. San  
519 Francisco, CA, United States.
- 520 Manchado, J.M., Sebastián, E., Romeral, J., Sobrado-Vallecillo, J., Herrero, P.L.,  
521 Compostizo, C., Gómez-Elvira, J., & Parro, V. (2015) SOLID SPU: A TRL 5-6  
522 Sample Preparation Instrument for Wet Chemistry Analysis on Mars. In Lunar  
523 and Planetary Science Conference. p. 1222.
- 524 Martins, Z. (2011) In situ biomarkers and the Life Marker Chip. *Astron. Geophys.*  
525 **52**(1), 1.34–1.35.
- 526 McKay, C.P. *et al.* (2013) The Icebreaker Life Mission to Mars: A Search for  
527 Biomolecular Evidence for Life. *Astrobiology*. **13**(4), 334–353.
- 528 McKay, D.S., Steele, A., Allen, C., Thomas-Keptra, K., Schweitzer, M.H., Priscu, J.,  
529 Sears, J., Avci, R., & Firman, K. (2000) Mars immunoassay life detection  
530 instrument (MILDI). *Lunar Planet Inst Contrib.* (1062 Part 2), 219–220.
- 531 McKenna-Lawlor, S., Gonçalves, P., Keating, A., Reitz, G., & Matthiä, D. (2012)  
532 Overview of energetic particle hazards during prospective manned missions to  
533 Mars. *Planet. Space Sci.* **63–64**(0), 123–132.
- 534 Moreau, T., Faye, C., Baqué, M., Desvignes, I., Coussot, G., Pascal, R., &  
535 Vandenaabeele-Trambouze, O. (2011) Antibody-based surfaces: Rapid  
536 characterization using two complementary colorimetric assays. *Anal. Chim.*  
537 *Acta*. **706**(2), 354–360.
- 538 Parro, V. *et al.* (2005) Instrument development to search for biomarkers on mars:  
539 Terrestrial acidophile, iron-powered chemolithoautotrophic communities as  
540 model systems. *Planet. Space Sci.* **53**(7), 729–737.
- 541 Parro, V. *et al.* (2008) SOLID2: an antibody array-based Life-detector instrument in a  
542 Mars drilling simulation experiment (MARTE). *Astrobiology*. **8**(5), 987–999.
- 543 Parro, V. *et al.* (2011a) Classification of Modern and Old Rio Tinto Sedimentary  
544 Deposits Through the Biomolecular Record Using a Life Marker Biochip:  
545 Implications for Detecting Life on Mars. *Astrobiology*. **11**(1), 29–44.
- 546 Parro, V. *et al.* (2011b) SOLID3: a multiplex antibody microarray-based optical sensor  
547 instrument for in situ Life detection in planetary exploration. *Astrobiology*.  
548 **11**(1), 15–28.
- 549 Le Postollec, A. *et al.* (2007) Development of a Biochip dedicated to planetary  
550 exploration. First step: resistance studies to space conditions. In *Journées SF2A*  
551 *2007 Semaine de l'Astrophysique Française 2007*.

- 552 Le Postollec, A. *et al.* (2009a) Monte Carlo Simulation of the Radiation Environment  
553 Encountered by a Biochip During a Space Mission to Mars. *Astrobiology*. **9**(3),  
554 311–323.
- 555 Le Postollec, A., Coussot, G., Baqué, M., Incerti, S., Desvignes, I., Moretto, P.,  
556 Dobrijevic, M., & Vandenabeele-Trambouze, O. (2009b) Investigation of  
557 Neutron Radiation Effects on Polyclonal Antibodies (IgG) and Fluorescein Dye  
558 for Astrobiological Applications. *Astrobiology*. **9**(7), 637–645.
- 559 Rabbow, E. *et al.* (2009) EXPOSE, an astrobiological exposure facility on the  
560 International Space Station - from proposal to flight. *Orig. Life Evol. Biospheres*.  
561 **39**(6), 581–598.
- 562 Rabbow, E. *et al.* (2012) EXPOSE-E: an ESA astrobiology mission 1.5 years in space.  
563 *Astrobiology*. **12**(5), 374–386.
- 564 Rabbow, E. *et al.* (2015) The astrobiological mission EXPOSE-R on board of the  
565 International Space Station. *Int. J. Astrobiol.* **14**(1), 3–16.
- 566 Sephton, M.A., Sims, M.R., Court, R.W., Luong, D., & Cullen, D.C. (2013) Searching  
567 for biomolecules on Mars: Considerations for operation of a life marker chip  
568 instrument. *Planet. Space Sci.* **86**, 66–74.
- 569 Sims, M., Cullen, D., Bannister, N., Grant, W., Henry, O., Jones, R., McKnight, D.,  
570 Thompson, D.P., & Wilson, P. (2005) The specific molecular identification of  
571 life experiment (SMILE). *Planet. Space Sci.* **53**(8), 781–791.
- 572 Sims, M.R. *et al.* (2012) Development status of the life marker chip instrument for  
573 ExoMars. *Planet. Space Sci.* **72**(1), 129–137.
- 574 Smith, H. & Parro, V. (2014) Planetary Protection Plan for an Antibody based  
575 instrument proposed for Mars2020. In 40th COSPAR Scientific Assembly. p.  
576 3140.
- 577 Sobrado, J.M., Martín-Soler, J., & Martín-Gago, J.A. (2014) Mimicking Mars: A  
578 vacuum simulation chamber for testing environmental instrumentation for Mars  
579 exploration. *Rev. Sci. Instrum.* **85**(3), 035111.
- 580 Vigier, F. *et al.* (2013) Preparation of the Biochip experiment on the EXPOSE-R2  
581 mission outside the International Space Station. *Adv. Space Res.* **52**(12), 2168–  
582 2179.
- 583 Wang, J. (2006) Electrochemical biosensors: Towards point-of-care cancer diagnostics.  
584 *Biosens. Bioelectron.* **21**(10), 1887–1892.
- 585 Zeitlin, C. *et al.* (2013) Measurements of Energetic Particle Radiation in Transit to  
586 Mars on the Mars Science Laboratory. *Science*. **340**(6136), 1080–1084.
- 587
- 588

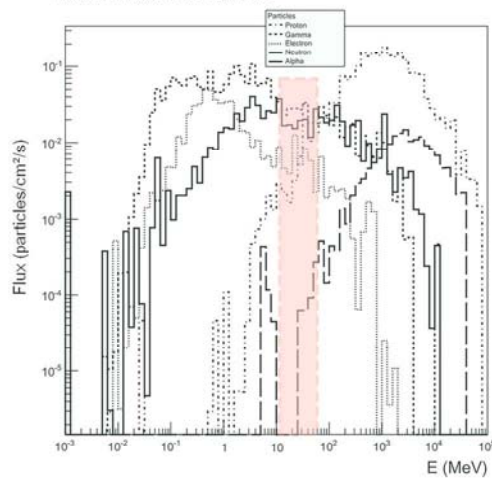
589 **Figure legends**

590 **Fig. 1:** Simulated spectra of particle fluxes, as a function of energy, during the Earth-  
591 Mars transit (left) and at Mars' surface (right) with the energy range of particles  
592 investigated in this study (red zone). This figure is an adaptation of Fig. 8 in Le  
593 Postollec *et al.* (2009a).

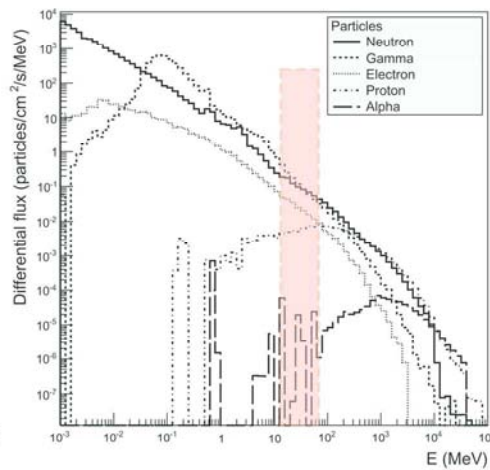
594 **Fig. 2: Top:** Proton irradiation using the Light Ion Facility (LIF) at the cyclotron of  
595 Louvain-la-Neuve. The source is located on the left in this picture and the samples are  
596 placed on the right behind a metal slide with a 10 cm diameter hole. Several removable  
597 disks are placed between the source and the samples to allow the modulation of protons  
598 energy. **Bottom Left:** Picture of the facility at the Institut Bergonié where samples were  
599 irradiated with 9 MeV electrons. **Bottom Right:** Mobile device developed to ensure the  
600 ELISA plate motion during carbon ions irradiation at LNS (Catania).



SIX MONTHS  
EARTH-MARS TRAVEL



ONE MONTH MARS STAY



**Tested particles and energies**  
 Proton: 15, 20, 25, 30, 50 MeV  
 Neutron: 17 MeV  
 Electron: 9 MeV  
 Carbon: 62 MeV/n

143x98mm (300 x 300 DPI)

Review



99x124mm (300 x 300 DPI)

**Table 1.** Influence of neutron, proton, electron and carbon radiation effects on grafted antibodies recognition capability at different fluences. The percentages of active antibodies were normalized using the NIC that were thus fixed at 100%. The percentage of antibodies receiving at least one particle was calculated according to the antibody surface density, the tested fluence and the sample geometry. SD, standard deviation;  $n$  is the number of measurements.  $p$ -value  $< 0.05$  (in bold) indicate samples that are different to NIC at 95 % of confidence.

	Protons						Neutrons	Electrons	$^{12}\text{C}$		
Fluence particles/cm <sup>2</sup>	$3 \times 10^{11}$		$3 \times 10^{12}$					$3 \times 10^{13}$	$2.3 \times 10^{11}$	$2.2 \times 10^6$	
Energy MeV	25	50	15	20	25	30	50	17 (mean energy)	9	62 MeV/n	
Antibodies receiving at least 1 particle % *	13		41					88	10	< 1	
Percentage of active antibodies % $\pm$ SD ( $n$ )	$84 \pm 9$ (13)	$89 \pm 10$ (5)	$97 \pm 19$ (15)	$62 \pm 7$ (5)	$65 \pm 12$ (13)	$73 \pm 8$ (5)	$92 \pm 14$ (5)	$100 \pm 7$ (4)	$96 \pm 4$ (5)	$98 \pm 4$ (4)	$102 \pm 10$ (10)
$p$ -value	<b><math>6.98 \times 10^{-4}</math></b>	0.083	0.612	<b><math>4.7 \times 10^{-4}</math></b>	<b><math>3.95 \times 10^{-8}</math></b>	<b><math>6.47 \times 10^{-4}</math></b>	0.283	0.938	0.136	0.656	0.839

\* Antibody surface density is equal to  $8.8 \times 10^{11}$  Ab/cm<sup>2</sup> for all experiments.

**Table 2.** Influence of neutron and proton irradiation on free-antibody recognition capability at different fluences. IC<sub>50</sub> ( $\mu\text{g}/\text{mL}$ ), half maximal inhibitory concentration; SD, standard deviation;  $n$  is the number of measurements. The percentages of active antibodies were estimated in comparison with NIC.  $p$ -values  $< 0.05$  (in bold) indicate samples that are different to non-irradiated controls at 95 % of confidence.

	Protons				Neutrons		Non-irradiated controls (NIC)
	$3 \times 10^{11}$		$3 \times 10^{12}$		$3 \times 10^{13}$		
Energy MeV	25	50	25	50	17 (mean energy)		
IC 50 ( $\mu\text{g}/\text{mL}$ ) $\pm$ SD (n)	$3.1 \pm 0.2$ (4)	$4.1 \pm 1.0$ (7)	$4.7 \pm 1.0$ (7)	$3.8 \pm 0.8$ (8)	$3.2 \pm 0.2$ (4)	$4.2 \pm 1.4$ (8)	$3.2 \pm 0.6$ (18)
Percentage of active antibodies %	100	71	50	79	105	73	100
$p$ -value	0.946	0.059	<b>0.004</b>	0.085	0.666	0.163	